JOURNAL OF Applied Polymer SCIENCE

Toughening of thermoset green zein resin: A comparison between natural rubber-based additives and plasticizers

Hamid Souzandeh, Anil N. Netravali
Fiber Science and Apparel Design, Cornell University, Ithaca, New York 14853-4401
Correspondence to: A. N. Netravali (E-mail: ann2@cornell.edu)

ABSTRACT: Zein-based brittle thermoset green resin was toughened using sorbitol, natural rubber fibers (NRF), and epoxidized natural rubber fibers (ENRF). NRF and ENRF were electrospun directly into zein slurry. Chemical, thermal, and mechanical properties of zein resin containing NRF (Zein/NRF) and ENRF (Zein/ENRF) were compared with those of sorbitol-plasticized zein. NRF was found to be immiscible in zein and Zein/NRF resins showed two distinct glass transition temperatures (T_g), whereas Zein/ENRF specimens showed significant increases in both T_g and degradation temperature (T_d) due to crosslinking between zein and epoxidized natural rubber. ENRF was more effective in enhancing fracture toughness of zein than NRF or sorbitol. Increased ENRF loading to 15 wt % showed significant increase in toughness with minimal decreases in strength and Young's modulus. Sorbitol and NRF were unable to improve the toughness of zein resin significantly. Environment-friendly zein/ENRF resin with higher fracture toughness developed in this study would be suitable in many applications including green composites. © 2019 Wiley Periodicals, Inc. J. Appl. Polym. Sci. **2019**, *136*, 48512.

KEYWORDS: biodegradable; biopolymers and renewable polymers; rubber; thermosets

Received 5 May 2019; accepted 17 August 2019
DOI: 10.1002/app.48512

INTRODUCTION

Zein protein has been recently used as a sustainable natural material in a wide variety of applications including resins for green composites, bioplastics, air filtration (in fiber form), food packaging (in film form), tissue engineering, and adhesive, due to its fully renewable and biodegradable nature and low cost.[1,2] However, in its pure form, it suffers from brittleness and low resistance to crack propagation. In particular, crosslinked thermoset zein resins have been shown to possess poor toughness and resistance to crack propagation.[2,3] Using plasticizers has been one of the most common methods to reduce the brittleness and improve the toughness of both bio-based as well as synthetic polymer resins. Plasticizers are small molecules that bring a large amount of free volume to the polymer system allowing easy molecular mobility and resulting in a lower glass transition temperature. However, one of the most common disadvantages of plasticization is leaching of the plasticizer with time that is accompanied with an increase in the brittleness of the polymers. As a result, many researchers have resorted to other methods such as addition of hybrid fibers, chemical modifications of the resin, or addition of ductile and/or tough materials to improve the toughness of brittle resins that are more permanent.[4,5] Among all these methods, toughening *via* dispersion of an elastomeric phase such as natural rubber (NR) in the polymer resin has been a promising method.[1] Plant-derived NR is also a biodegradable and fully sustainable material, which possesses moderate tensile strength but good tear resistance, toughness, and high resilience.[6] Due to its very low glass transition temperature (T_g) of about −65 °C and flexible backbone structure, NR is highly extensible at room temperature and makes it a desirable candidate for toughening purposes.[1] However, NR suffers from a few disadvantages including high hydrophobicity, poor environmental and oil resistance, and poor miscibility with many resins that cause severe difficulties in obtaining uniform dispersion of NR in resins and, as a result, significantly reduces the tensile properties of resins and also limits its use for polymer resin-toughening applications.[1,7]

To improve the toughness of a brittle polymer resin by adding rubber materials, in addition to uniform dispersion, it is extremely important to obtain good interfacial bonding *via* chemical interactions between the resin and the rubber.[8–10] For that reason, researchers have incorporated certain functional groups in the rubber structure. Recently, epoxidized (epoxy functionalized) natural rubber (ENR) has attracted significant interest in the area of advanced composites.[11,12] Many studies have reported successful toughening of polymeric resins such as poly(D,L-lactic acid), poly (3-hydroxybutyrate-*co*-3-hydroxyvalerate),[13] and soy protein using ENR.[1,14] The enhanced interfacial bonding via hydrogen

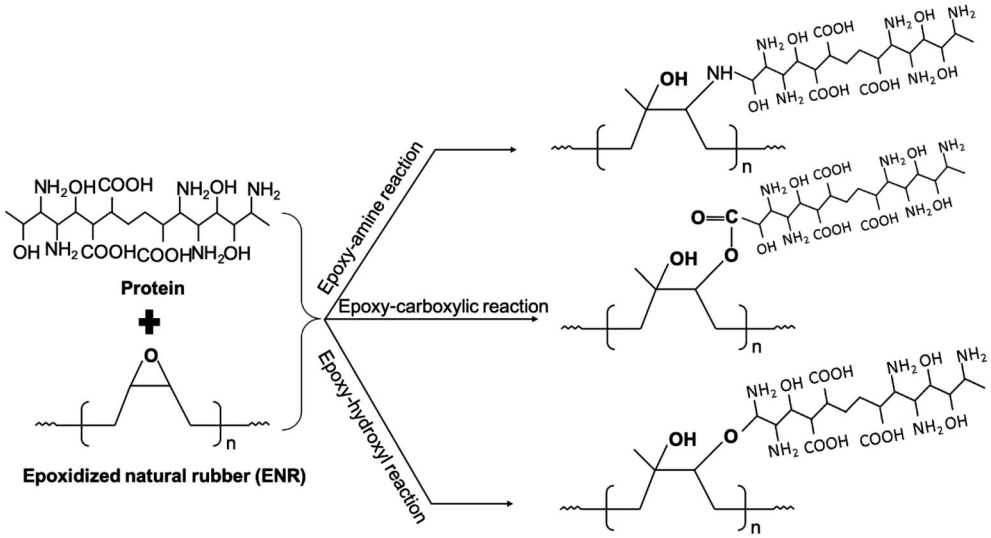

Figure 1. Possible reactions between amine, carboxyl, and hydroxyl groups from zein and epoxy groups from ENR.

bonding between soy protein isolate (SPI) and ENR was reported to be the reason for the improved toughness of the polymer resin.[15] The epoxy groups in ENR have been confirmed to react with amine and carboxyl groups in the polymer resin forming covalent linkages between the two.[14,16] Figure 1 shows possible interactions between epoxy groups in ENR and amine, carboxyl, and hydroxyl groups existing in the amino acids, such as lysine, glutamic acid, and serine, of zein protein during the curing process of zein (around 100 °C) as the ENR epoxy ring opens up. These reactions are consistent with that of the ENR-toughened soy protein resin reported earlier by Kim and Netravali.[1] Further, hydroxyl groups in zein could also react with the epoxide groups in ENR.[17,18] As a result, ENR is thought to be a promising material to improve the toughness of the brittle zein resin.

In recent years, polymeric fibers have been used in many diverse applications due to their excellent mechanical and physical properties, particularly their high surface area-to-volume ratio.[19] Fibers possess diameters ranging from a few nanometers to several micrometers depending on how they are made and the applications they are intended for.[20] Many different techniques including extrusion, gel-spinning, electrospinning, force spinning, and so on, have been used to spin polymeric fibers of different diameters as needed for the applications.[21] Among all these fiber production methods, electrospinning has been most commonly used to spin a wide variety of polymers, particularly when a broad range of submicrometer-sized diameters are needed.[22,23] The electrospinning process typically includes a high-voltage supply, a syringe pump and needle, and a conductive collector such as metal.[24] Most commonly, the positive electrode is connected to the syringe needle through which the polymer solution is pumped and the metal collector is grounded. A high voltage, several (5–30) thousand volts, is applied to the needle that charges the polymer solution coming out. When the electrostatic repulsion overcomes the surface tension of the viscous polymer solution emerging from the needle, the polymer is pushed or ejected toward the conductive collector and deposited in the form of fine fibers.[25] The fibers, when deposited, are mostly in the solid form as a result of fast evaporation of the solvent.[25] Many parameters such as polymer concentration, solution viscosity and flow rate, surface tension, applied voltage, needle-to-collector distance, and so on, can influence the properties of electrospun fibers including their diameters.[26] For example, higher polymer concentration increases the viscosity and results in larger diameter fibers. In addition, higher needle-to-collector distance allows splitting or stretching of fibers making the diameters of the fibers smaller. Only few research studies have reported electrospinning of rubber materials due to the poor fiber formation property of rubbers caused by the inefficiency of conventional solvent systems available for the dissolution of rubbers.[27,28] Only a few studies have successfully spun synthetic cis-1,4-polyisoprene,[29] polybutadiene rubber,[30] ENR,[14] and blends of NR with polycaprolactone or acrylonitrile butadiene styrene [27] fibers via electrospinning.

This paper compares the effectiveness of three methods, namely sorbitol plasticization and electrospun natural rubber fibers (NRFs) and epoxidized natural rubber fibers (ENRFs), as toughness-enhancing mechanisms for crosslinked zein resin that may be used as a green resin in composites. While sorbitol was directly added to zein, NR and ENR were dissolved in chloroform ($CHCl_3$), a relatively efficient and green solvent, and the fibers were spun directly into zein resin slurry with different loadings, following the process previously employed by Kim and Netravali.[14] The toughening agent (sorbitol, NR, and ENR) loadings were varied from 0 to 20% based on the weight of zein. Further, the effects of toughening agent loading on the chemical, thermal, and mechanical properties, particularly toughness, of the zein resin were studied.

EXPERIMENTAL

Materials

Zein protein from maize (powder), D-sorbitol (plasticizer), chloroform, and analytical glutaraldehyde (GA, 25 wt % in water) as a crosslinking agent were purchased from Sigma Aldrich Chemical Co., St. Louis, MO. Ethanol (EtOH, 99% purity) was obtained from Fisher Scientific, (Pittsburgh, PA). NR and ENR (50 mol % conversion) were obtained from Malaysian Rubber Board, Kuala

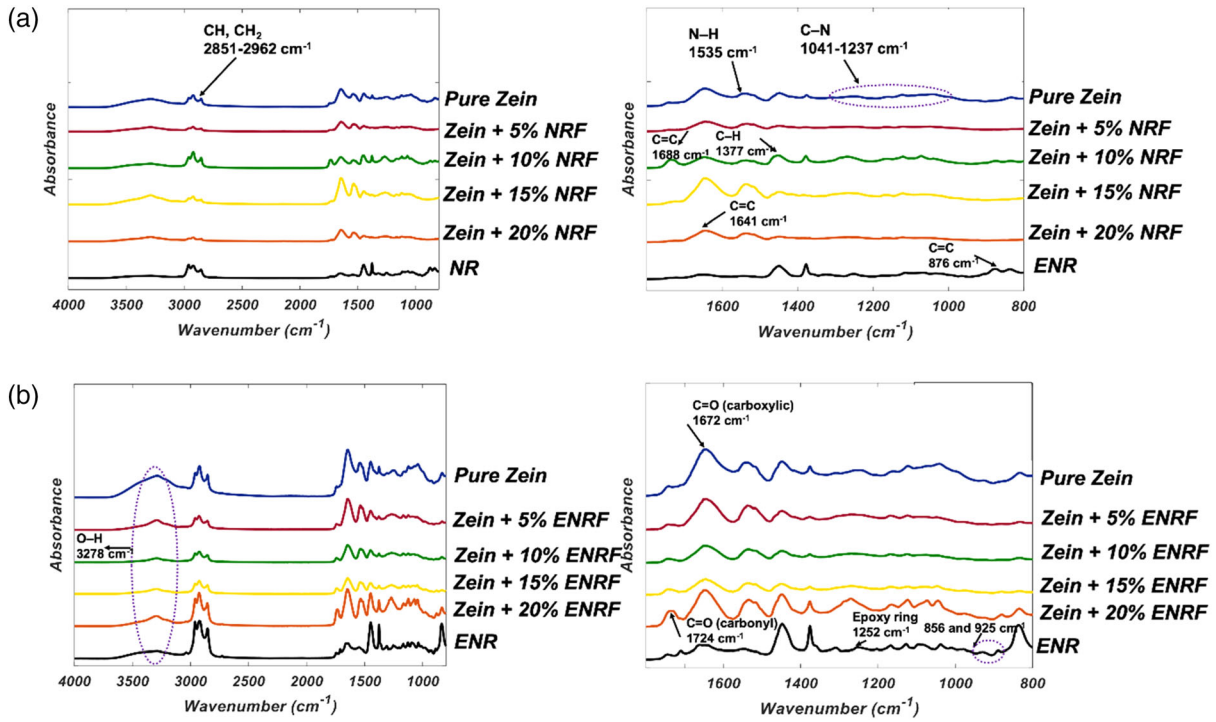

Figure 2. ATR–FTIR spectra of (a) Zein/NRF and (b) Zein/ENRF for all loadings (0, 5, 10, 15, 20, and 100 wt %). [Color figure can be viewed at wileyonlinelibrary.com]

Lumpur, Malaysia. All chemicals were utilized as received without further purification.

Wet Electrospinning of Rubber Materials

NR and ENR were dissolved in chloroform at a concentration of 2% (w/v) and stirred overnight at 30 °C. The solutions were then filled into a 30-mL syringe and electrospun into fibers using the Gamma power supply at a high voltage of 16 kV. The solution feeding rate was set to 100 and 500 μL/min for NR and ENR, respectively, and the needle-to-collector distance was fixed at 15 cm. Zein resin solution in aqueous ethanol (20 w/v%) was prepared in a beaker, which was then placed on the aluminum collector (distance to needle = 22 cm), such that the distance from resin surface to needle was maintained at 15 cm. NR and ENR fibers were directly electrospun into the zein resin that was being stirred continuously at 200 rpm using a magnetic stirrer to prevent any aggregation of electrospun fibers.

Preparation of Toughened Zein Resin

Zein protein powder was mixed with aqueous ethanol (85 vol %) and the solution was stirred for 1 h at 500 rpm at 50 °C to obtain a 20 w/v% zein solution. GA, as the crosslinking agent, was then added to the mixture (10 wt % based on zein powder) and stirred for another 1 h. The zein-GA crosslinking reaction is fast and viscosity increases quickly. In order to study the effects of the plasticizer on the mechanical properties of the resin, the plasticizer (sorbitol) content was varied between 0 and 20%, in steps of 5%, based on the weight of the zein. Electrospun NR and ENR fibers (NRFs, ENRFs) using the 2% solution, as mentioned earlier, were directly deposited into the zein resin that was being stirred continuously. Their loadings also varied from 5 to 20 wt %, based on the weight of the zein. Zein resins containing different loadings of sorbitol plasticizer, NRFs, or ENRFs were cast in a Teflon-coated glass mold (15 cm × 15 cm) and dried and precured at 60 °C in an air-circulating oven for 72 h to form sheets. The dried films taken from the molds were then cured in a hot press at 95 °C and under a pressure of 0.5 MPa for 20 min to complete the zein-GA crosslinking reaction. All resin sheets having 1–1.5 mm thickness were conditioned at 21 °C and 65% relative humidity (RH) level for 72 h prior to any characterization.

Tensile Properties of Toughened Zein Resins

Conditioned zein resin sheets of all compositions were laser cut to obtain the tensile test specimens with dimensions of 100 mm (L) × 10 mm (W). Tensile properties such as fracture stress, fracture strain, toughness, and Young's modulus of control and toughened zein specimens were characterized using an Instron universal testing machine (Instron, Model 5566, Instron Co., Canton, MA) according to ASTM D882-02. Gauge length of 50 mm and crosshead speed of 10 mm/min (strain rate of 0.2 min^{-1}) were maintained for all tensile tests. Five specimens were tested for each condition to ensure the reproducibility of the results.

Thermal Analysis of Rubber-Toughened Zein Resins

Differential scanning calorimetry (DSC) (TA-DSC 2000, TA instrument Inc., New Castle, DE) was conducted at a heating rate of 10 °C/min from −80 to 300 °C to evaluate any changes in the thermal properties of rubber-toughed zein resin. All DSC tests were performed in a nitrogen environment (flow rate of 50 mL/min). Thermogravimetric analysis (TGA) of control and rubber-toughened zein resin specimens was performed using a

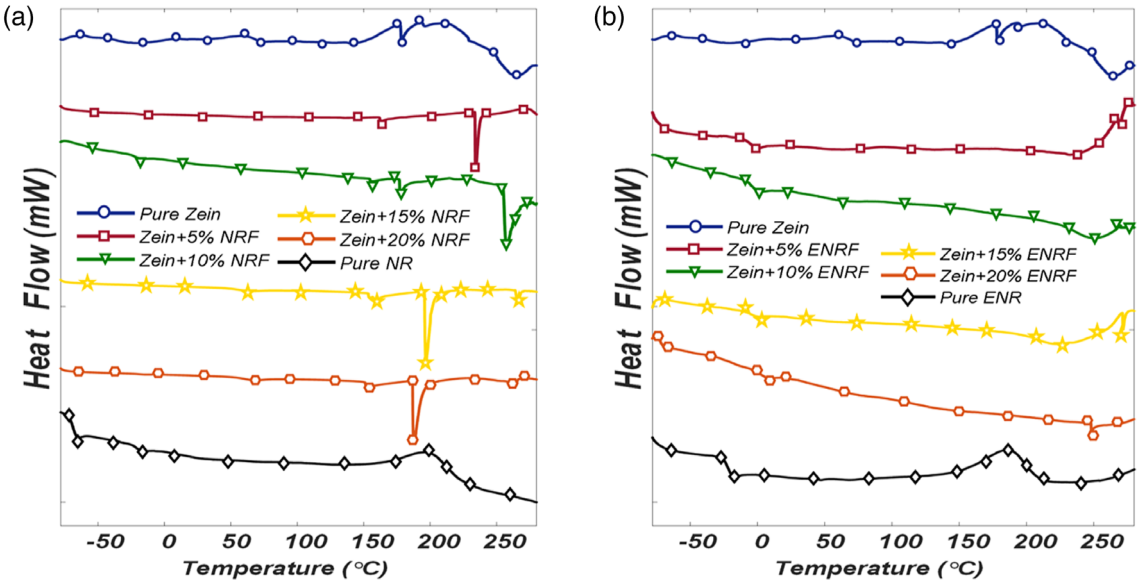

Figure 3. DSC thermograms of (a) Zein/NRF and (b) Zein/ENRF specimens with different rubber fiber loadings. [Color figure can be viewed at wileyonlinelibrary.com]

thermogravimetric analyzer (TA-TGA Q500, TA Instruments, Inc., New Castle, DE). The specimens were tested at a heating rate of 10 °C/min from 30 to 600 °C under a nitrogen environment (flow rate of 60 mL/min).

Zein Resin Characterization

A scanning electron microscope (SEM), LEO 1550 FESEM, was utilized to characterize the microstructure of the fracture surfaces of control and toughened zein resin specimens. Attenuated total reflectance Fourier-transform infrared spectroscopy (ATR-FTIR spectrometer, Frontier, Perkin Elmer, Waltham, MA) was utilized to characterize the chemical composition of control and rubber-toughened zein specimens. The tests were conducted from 4000 to 800 cm^{-1} wavenumbers with a total of 32 scans and a resolution of 4 cm^{-1}.

RESULTS AND DISCUSSION

Chemical Analysis of Rubber-Toughened Zein Resins

Figure 2 shows the ATR-FTIR spectra of control and NRF and ENRF-toughened zein resins for all loadings (0, 5, 10, 15, and 20 wt %) as well as pure NRF and ENRF. It can be seen from Figure 2 that pure zein showed absorption peaks at 1041–1237, 1535, 1672, and 2851–2962 cm^{-1} (wavenumbers) corresponding to C—N stretching, N—H stretching, C═O stretching, and CH and CH_3 asymmetric stretching, respectively.[31–36] Similar infrared absorption peaks have been reported by other researchers for zein resin.[31,32] After the addition of NRF, new peaks at 1641 and 1688 cm^{-1} representing C═C stretching from NR [shown in Figure 2(a)] were observed.[12] However, Figure 2(b) indicates that addition of ENRF results in peaks at 856, 925, and 1252 cm^{-1} corresponding to epoxide groups present in ENRF.[16,26,37]

As mentioned earlier (also shown in Figure 1), the epoxy groups in ENRF can react with carboxylic groups (COOH) present in the amino acids, such as glutamic acid and aspartic acid, of zein resin leading to the formation of ester crosslinks during the curing process (hot-pressing at 95 °C).[38] As can be seen in Figure 2(b), an absorption peak around 1724 cm^{-1} was observed in the spectra of Zein/ENRF specimens, which corresponds to an ester carbonyl group (C═O). It is noted that a similar peak was obtained for control and Zein/NRF specimens as well and is related to the amine–aldehyde crosslinking reaction between protein and GA.[39,40] However, the intensity of the carbonyl peak at 1724 cm^{-1} was significantly higher with ENRF loading. Since NRF does not undergo the esterification reaction with zein, only the small carbonyl peak caused by crosslinking reaction between zein and GA was observed, as shown in Figure 2(a). Further, broad peaks around 3300–3500 cm^{-1} seen in Figure 2(a,b) represent the existence of hydroxyl groups (—OH) from various amino acids. These absorption peaks can be due to the reaction between amine groups of zein, such as lysine and arginine and epoxy groups of ENRF, as discussed earlier (Figure 1), which leads to the generation of the hydroxyl groups. In addition, the hydroxyl groups in zein can also react with the epoxide groups in ENR to form secondary hydroxyl groups.[17,18,41] Presence of hydroxyl groups in all specimens also attract additional moisture and were conditioned at 65% RH for 72 h.

Thermal Properties of Toughened Zein Resins

Figure 3 shows DSC thermograms of Zein/NRF and Zein/ENRF specimens, with different compositions, from −80 to 300 °C. It can be seen that all specimens showed an endothermic peak between 70 and 150 °C. This peak is believed to be due to the loss of volatile components, primarily absorbed water, as well as breakdown of hydrogen bonds in the zein structure that results in chain relaxation.[42–45] An endothermic transition around 168 °C observed in the DSC thermogram for pure zein specimen shown in Figure 3 is associated with its glass transition temperature (T_g).[42,46,47] Above this temperature, zein chains have mobility. These results are consistent with earlier studies on thermal properties of zein films.[42,46,47] It can also be seen from Figure 3

Table I. Glass Transition (T_g) and Degradation Temperature (T_d) of Zein/NRF and Zein/ENRF Specimens for All Rubber Fiber Loadings, Using DSC and TGA-DTGA Technique

Specimens	Toughening agent loading(wt %)	DSC	TGA-DTG
		T_g (°C)	T_d (°C)
Zein/NRF	0	181	304
	5	-56, 183	304
	10	-55, 196	301
	15	-55, 194	297, 365
	20	-51, 203	298, 381
	100	–58	387
Zein/ENRF	0	181	304
	5	-12	313, 361
	10	-8	318, 365
	15	-3	323, 361
	20	15	327, 359
	100	-27	368

(a) that the thermogram for pure NR shows an endothermic transition for T_g at around −58 °C. All Zein/NRF specimens showed two transition points for T_g, first around −54 °C, corresponding to NR, and the second between 160 and 230 °C corresponding to zein resin (summarized in Table I). It should be noted that due to the poor electrospinning behavior, NR was deposited into the zein resin both in fiber and gel particle forms. In addition, because of the immiscibility between zein and NRF or NR, they remain phase-separated and show their elastic state while zein stays in its glassy state until its T_g at around 200 °C. Since no crosslinking reaction was anticipated between zein and NRF, two separate T_gs were observed for Zein/NRF specimens. For pure ENR specimen, a T_g in the range of −27 °C was observed [as seen in Figure 3(b)], much higher than −58 °C obtained for NR. All Zein/ENRF specimens showed an increase in T_g from −12 to 15 °C as the ENR loading increased from 5 to 20 wt %. No such trend was obtained for Zein/NRF specimens. This increase in T_g for Zein/ENRF specimens is the further confirmation of the crosslinking between the epoxy groups of ENR and the amino acids of zein. These phenomena are consistent with the study on NR and ENR toughening of SPI resin reported earlier by Kim and Netravali.[1,14]

Figures 4 and 5 show the TGA and DTA (first derivative of TGA curve) thermograms of Zein/NRF and Zein/ENRF specimens for all loadings, from 30 to 600 °C. It can be seen from these thermograms that for pure zein resin, the initial weight loss that occurs up to 130 °C corresponds to the evaporation of the absorbed moisture and any residual solvent. Weight loss from 130 to 200 °C, about 10%, can be partially attributed to the evaporation of fatty acids.[45] The main degradation temperature (T_d) of pure zein resin was observed at about 304 °C, as shown in Figure 4(a), and confirms the earlier literature.[45,48,49] Figure 4(f) shows T_d, represented by sharp and significant weight loss, at about 387 °C for pure NR. The T_d of Zein/NRF specimens slightly reduced from 304 to 298 °C with NRF loading [Figures 4(b–e) and Table I]. Because of the nonuniform dispersion of NRF in zein resin, as mentioned earlier, the specimens consisted of phase-separated domains. Even with the phase separation, specimens with lower NRF loadings (5 and 10 wt %) showed only one degradation peak corresponding to zein resin. However, in the case of higher loadings of 15 and 20 wt %, two separate degradation peaks were observed around 298 and 380 °C corresponding to zein resin and NRF, respectively. On the other hand, it can be seen from Figures 5(b–e) that the degradation temperature of Zein/ENRF specimens increased from 313 to 327 °C when the ENRF loading increased from 5 to 20 wt %. As in the case of T_g, the increase in T_d of Zein/ENRF specimens is attributed to the crosslinking between epoxy groups of ENR and amine groups present (also COOH and OH) in zein, as discussed earlier. Additionally, a second degradation peak around 360 °C was observed for all Zein/ENRF specimens [Figure 5(b–e)], which is believed to be related to the non-crosslinked ENRF in the resin. This is consistent with the thermogram of pure ENR presented in Figure 5(f) that shows the T_d around 368 °C.

Tensile Properties and Fracture Morphology of Toughened Zein Resins

Figure 6 shows typical tensile stress–strain plots for control (pure) and toughened zein resins using sorbitol (plasticizer), NRF, and ENRF. Table II summarizes the tensile properties of the toughened zein resins. It can be seen from Figure 6(a) and Table II that as the sorbitol content increased from 0 to 20 wt%, the Young's modulus and fracture stress decreased significantly from 979.5 to 45.4 MPa and from 11.6 to 2.2 MPa, respectively. On the other hand, the fracture strain increased from 2.03 to 50.2% and toughness increased from 0.14 to 1.18 MPa. These results are consistent with the reported effect of sorbitol as a plasticizer.[50] Although the addition of sorbitol resulted in the enhancement of the toughness of zein resin, this effect can be expected to wear off over time due to the leaching of sorbitol from the resin, as discussed earlier. As can be seen from stress–strain plots in Figure 6(b) and data in Table II, adding 20-wt % NRF to zein resin increased the fracture strain and toughness from 2.03 to 68.6% and 0.14 to 1.45 MPa, respectively. However, at the same time, Young's modulus and fracture stress reduced significantly from 979.5 to 69.7 MPa and 11.85 to 1.22 MPa, respectively, as was expected. Stress–strain plots for Zein/ENRF in Figure 6(c) and data in Table II indicate that the increase in ENRF loading from 0 to 15 wt % increased the fracture strain from 2.03 to 73.26% and toughness from 0.14 to 5.20 MPa, while the fracture stress and Young's modulus decreased from 11.58 to 6.31 MPa and 979.50 to 141.32, respectively. It can also be seen from data summarized in Table II that all Zein/NRF specimens have lower fracture strain than Zein/ENRF specimens. It has been reported that the neat NR and ENR used in this study had fracture strains of about 400 and 190%, respectively.[1,14] Due to the poor solubility of NR in chloroform that resulted in its poor electrospinning behavior, NR was deposited into the zein resin both in fiber as well as gel particle forms, which caused non-uniformity in the dispersion of NR along with phase separation. Technically, the Zein/NRF specimens were expected to show higher fracture strains than Zein/ENRF specimens. However, in

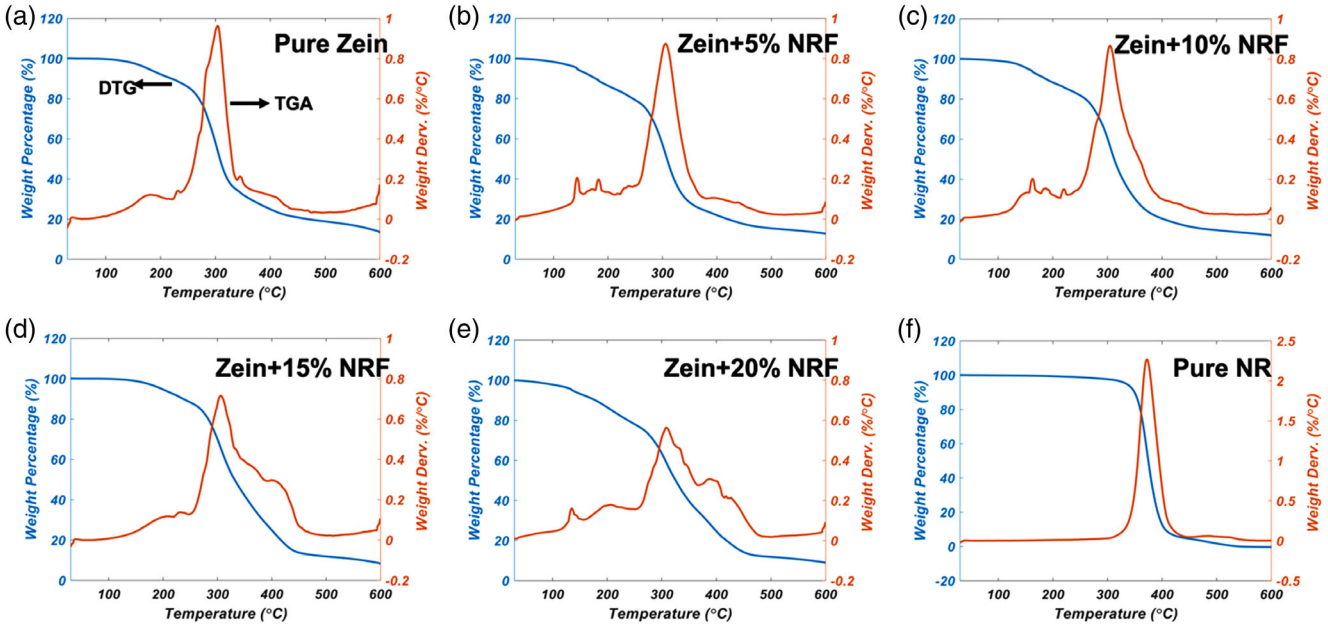

Figure 4. TGA and DTA thermograms of Zein/NRF specimens with NRF loadings of (a) 0, (b) 5, (c) 10, (d) 15, (e) 20, and (f) 100%. [Color figure can be viewed at wileyonlinelibrary.com]

addition to poor mechanical properties of NR, immiscibility and poor dispersion of NR in zein resin were believed to be the main reasons for the Zein/NRF specimens possessing a substantial lower fracture stress, Young's modulus, and fracture strain than that of the Zein/ENRF specimens.

In comparison, all Zein/ENRF specimens resulted in significantly higher toughness values than the Zein/NRF and sorbitol plasticized specimens. For instance, the specimens with 10–wt % ENRF showed a toughness value of 4.18 MPa, while the specimens with the same loading of NRF and sorbitol resulted in toughness values of only 1.14 and 0.89 MPa, respectively. It is well known that the bonding between the resin and the reinforcement is the key factor to enhance the mechanical properties of a composite. Similarly, as discussed earlier, the epoxy groups of ENR react with amine, carboxyl, and hydroxyl groups present in zein structure resulting in the formation of a three-dimensional network. It is believed that the formation of the crosslinks between zein and ENRF led to higher fracture strain and stress as well as Young's modulus than that of sorbitol and NRF-toughened resins where no such possibility exists.[51,52] The increased fracture strain combined with higher modulus in

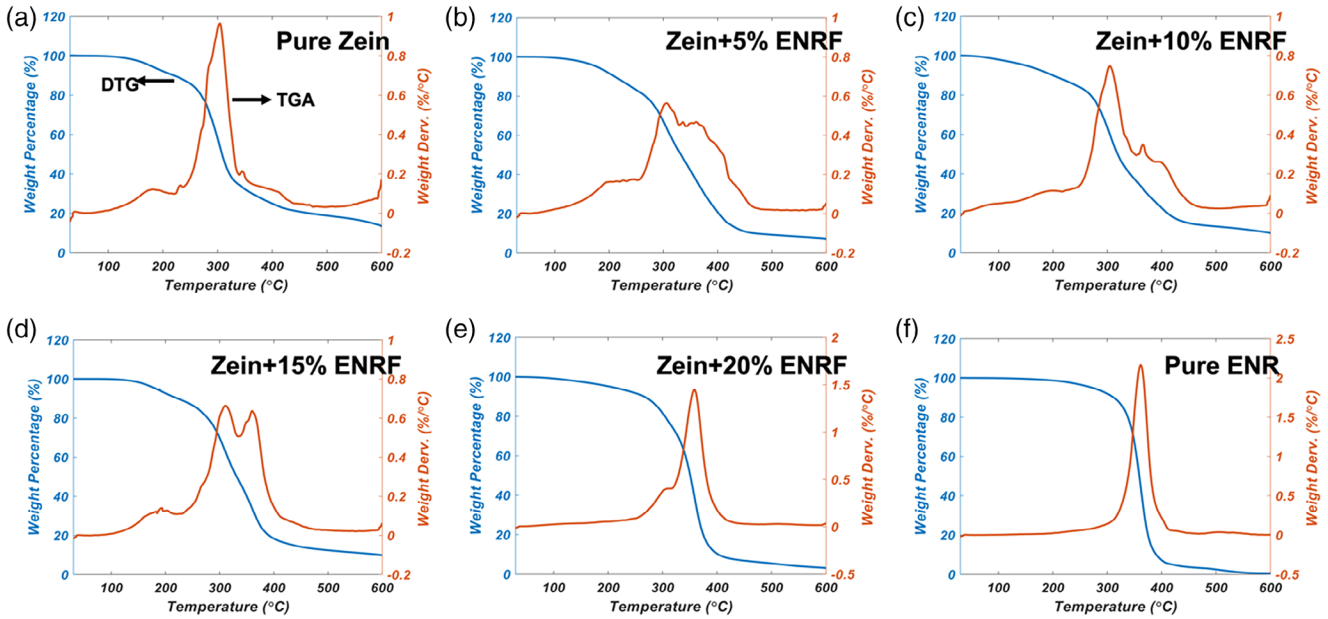

Figure 5. TGA and DTA thermograms of Zein/ENRF specimens with ENRF loadings of (a) 0, (b) 5, (c) 10, (d) 15, (e) 20, and (f) 100%. [Color figure can be viewed at wileyonlinelibrary.com]

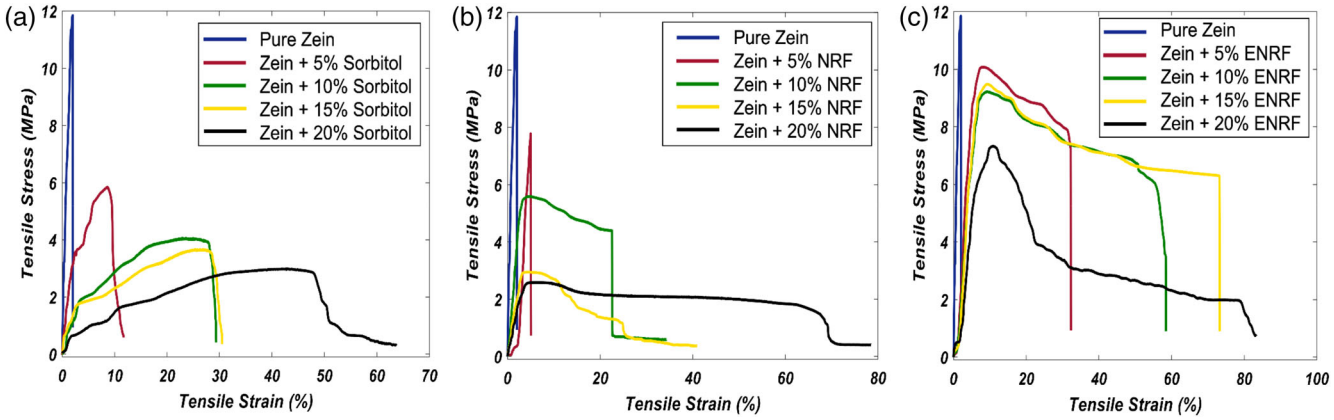

Figure 6. Typical tensile stress–strain plots of toughened zein resins with different loadings of (a) sorbitol plasticizer, (b) NRF, and (c) ENRF. [Color figure can be viewed at wileyonlinelibrary.com]

ENRF-toughened zein resins can significantly increase the energy absorbed during tensile deformation and increase the toughness compared with that of Zein/NRF and sorbitol-plasticized specimens.[53] These results also demonstrate that the tensile properties of Zein/ENRF specimens decreased when ENRF loading increased further above 15 wt %. This is believed to be because of the dominant influence of ENR in increasing the flexibility as well as somewhat less than desired dispersion of ENRF due to their significant entanglement while electrospinning. With increased loading of ENRF from 15 to 20 wt %, the fracture stress, Young's modulus, and toughness decreased further from 6.31 to 2.06, 141.3 to 138.7, and 5.20 to 2.73 MPa, respectively. This behavior is consistent with the reported results in other research on ENR toughening of epoxy resins.[52]

Figure 7 shows SEM typical images of specimen and fracture surfaces of Zein/NRF and Zein/ENRF specimens with 15-wt % loading. Many cracks can be seen on the surface of both NRF and ENRF-toughened specimens after tensile testing. Figure 7(a–c) shows the SEM images of the Zein/NRF specimen surface after tensile testing. It can be seen that NR fibers form bridges and keep the two pieces of the resin specimen together. This is because the fracture strain of NR (about 400%) is many times that of zein (about 2%). Even when the specimen fractures, the NR fibers with high aspect ratio do not break and they simply stretch. This results in an increase in the toughness and a decrease in the brittle nature of the Zein/NRF specimens. These results were confirmed by the tensile stress–strain data for the Zein/NRF specimens, as discussed earlier. However, from the SEM image of the fracture surface of Zein/NRF specimen shown in Figure 7(d), both broken NR fibers (cross section) and rubber particles can be observed. Phase separation and weak interaction between NR and zein resin can also be observed from Figure 7 (d), which is in line with the thermal behavior of Zein/NRF specimens as discussed earlier. On the other hand, SEM images of

Table II. Tensile Properties of Toughened Zein Resins

Specimen	Toughening agent loading (wt %)	Fracture stress (MPa)	Fracture strain (%)	Young's modulus (MPa)	Toughness (MPa)
Zein/sorbitol	0	11.85 ± 0.6[a]	2.03 ± 0.3	979.5 ± 8.7	0.14 ± 0.02
	5	5.76 ± 0.8	8.88 ± 1.6	227.5 ± 4.4	0.44 ± 0.06
	10	3.88 ± 0.8	27.93 ± 1.5	47.4 ± 5.2	0.89 ± 0.09
	15	3.58 ± 0.4	28.23 ± 1.1	46.5 ± 2.1	0.81 ± 0.1
	20	2.18 ± 1.1	50.22 ± 1.8	45.4 ± 2.7	1.18 ± 0.04
Zein/NRF	0	11.85 ± 0.6	2.03 ± 0.3	979.5 ± 8.7	0.14 ± 0.02
	5	7.77 ± 1.2	5.14 ± 1.1	256.8 ± 5.4	0.12 ± 0.05
	10	4.39 ± 0.9	22.58 ± 1.9	192.9 ± 5.9	1.14 ± 0.07
	15	1.17 ± 0.5	24.71 ± 1.7	82.9 ± 4.1	0.98 ± 0.07
	20	1.22 ± 0.8	68.58 ± 1.6	69.7 ± 3.7	1.45 ± 0.12
Zein ENRF	0	11.85 ± 0.6	2.03 ± 0.3	979.5 ± 8.7	0.14 ± 0.02
	5	7.87 ± 0.5	31.33 ± 0.9	292.8 ± 4.1	2.64 ± 0.11
	10	6.81 ± 0.4	49.51 ± 1.1	199.2 ± 3.6	4.18 ± 0.09
	15	6.31 ± 0.7	73.26 ± 1.3	141.3 ± 4.3	5.20 ± 0.26
	20	2.06 ± 1.1	79.88 ± 1.4	138.7 ± 2.1	2.73 ± 0.08

[a] Standard deviation is reported for all data.

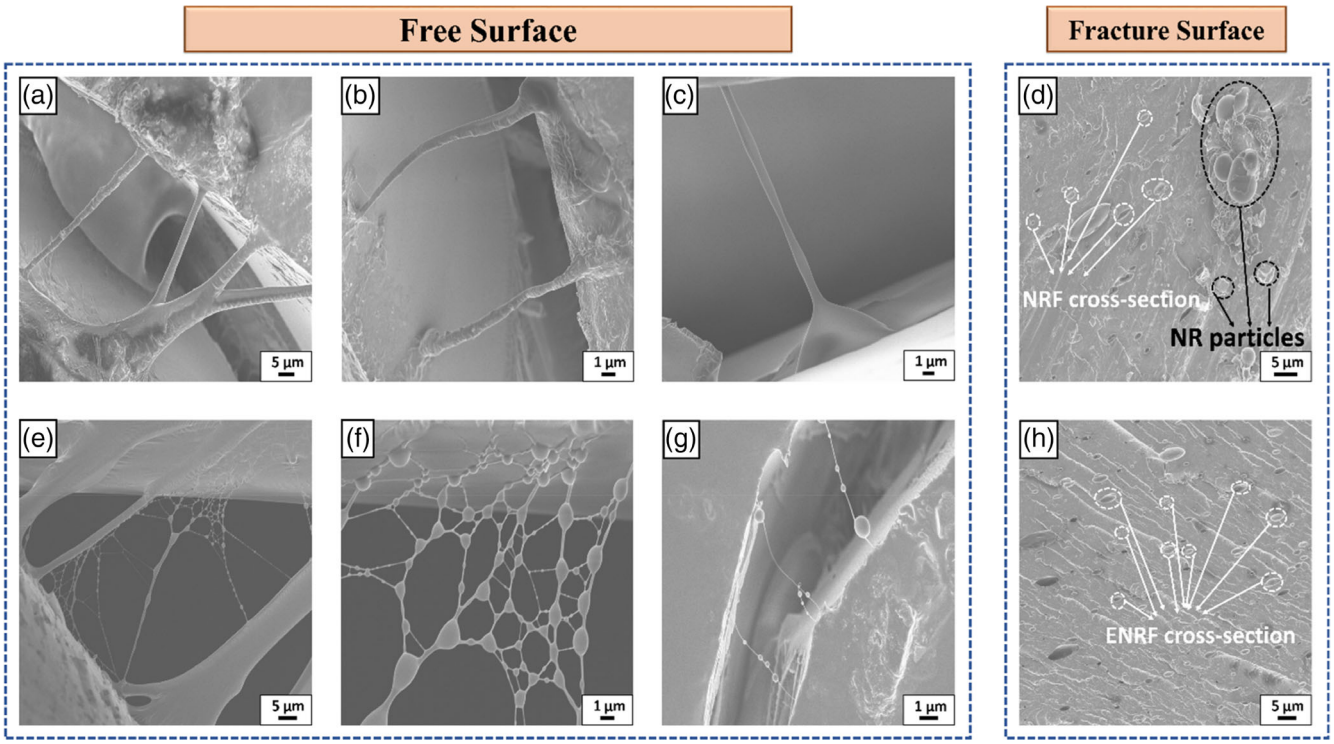

Figure 7. SEM images of (a–c) specimen surface after testing and (d) tensile fracture surface of Zein/NRF specimen with 15-wt % NRF loading. SEM images of (e–g) specimen surface after testing and (h) tensile fracture surface of Zein/ENRF specimen with 15-wt % ENRF loading. [Color figure can be viewed at wileyonlinelibrary.com]

fracture surfaces of Zein/ENRF presented in Figures 7(e–g) clearly show the fiber network bridging the cracks created during the tensile testing. It was observed that during electrospinning, ENR fibers were formed in much smaller average diameters (about 0.67 μm), compared with NR fibers (about 2.48 μm). ENR fibers were also in the form of fiber networks. This network structure significantly helps with the toughening of the resin as shown in Figure 7(c). Moreover, no noticeable phase separation was found for the Zein/ENRF specimens. This has been confirmed by the DSC results discussed earlier. From the typical fracture surface of Zein/ENRF specimen, shown in Figure 7(h), only fiber cross sections can be observed. This indicates that the ENR fibers have very good interaction with zein resin; therefore, very few holes were observed that suggest almost no fiber pull-out phenomenon. This is clearly due to the crosslinking between ENR and zein resin. These results are consistent with the tensile and thermal behavior of Zein/ENRF specimens, as discussed earlier.

CONCLUSIONS

Results of this study clearly indicate that the toughness of originally brittle thermoset zein resin can be enhanced significantly by mixing electrospun NR and ENR fibers. The fibers can be mixed in the resin while being electrospun. The mechanical properties, particularly toughness, of the rubber-toughened zein resins with the sorbitol plasticized resin show that zein resin toughening by NR is more efficient than sorbitol plasticization. The results also demonstrate that ENR fibers are significantly more effective in toughening of zein resin than NR fibers. Toughening of zein resin by ENR fibers resulted in higher Young's modulus and tensile strength than that of NR fiber-toughened resins. The enhanced tensile properties of ENRF-toughened zein resin were primarily due to the crosslinking between epoxy groups in ENR and amine and carboxyl groups in zein during the curing process carried out by hot pressing. These reactions were investigated through ATR-FTIR. However, crosslinking may also happen between the epoxide groups in ENR and amine and hydroxyl groups in zein. DSC results indicated that all Zein/NRF specimens showed two distinctive T_g values around −55 and 185 °C representing the T_g of NR and zein, respectively. This result alongside with T_d of Zein/NRF specimens proved that only weak interactions exist between NR and zein. On the other hand, for Zein/ENRF specimens, as the ENRF loading was increased from 5 to 20 wt %, an increase in T_g (from −12 to 15 °C) and T_d (from 313 to 327 °C) were observed. Additionally, the tensile properties demonstrated that the addition of NRF and ENRF to zein resin improved its toughness more effectively than sorbitol plasticization. Zein/ENRF specimens with 15-wt % loading of ENR fibers resulted in a significant improvement in the toughness value of zein resin from 0.14 (control) to 5.20 MPa. This is in comparison with sorbitol plasticized resin (0.81 MPa) and NRF toughened resin (0.58 MPa) with the same loading. Zein/ENRF specimens also showed the highest tensile strength and Young's modulus. These improvements in mechanical properties of zein resin were predominantly due to the crosslinking between ENR and zein while no such reactions were expected for NR and sorbitol. This study shows that the small diameter electrospun ENR fibers could be a promising solution to enhancing thermal and mechanical

properties, particularly toughness, of the green zein resin. Enhanced properties can help broaden the usage of this green resin in many applications, primarily the green composites.

ACKNOWLEDGMENTS

This work was supported by the National Institute of Food and Agriculture (NIFA), U.S. Department of Agriculture (Multistate Research Project S-1054 under 1 004 862). In addition, partial support from NSF-CREST grant (1137681) was used. The authors would like to acknowledge support of the Cornell Center for Materials Research (CCMR) shared facilities supported through the NSF MRSEC program (DMR-1719875) and the Department of Fiber Science & Apparel Design facilities.

REFERENCES

1. Kim, J. R.; Netravali, A. N. *J. Appl. Polym. Sci.* **2017**, *134*, 1.
2. Huo, W.; Wei, D.; Zhu, W.; Li, Z.; Jiang, Y. *J. Cereal Sci.* **2018**, *79*, 354.
3. Ghanbarzadeh, B.; Oromiehie, A. R.; Musavi, M.; D-Jomeh, Z. E.; Rad, E. R.; Milani, J. *Food Res. Int.* **2006**, *39*, 882.
4. Mehta, G.; Mohanty, A. K.; Misra, M.; Drzal, L. T. *Green Chem.* **2004**, *6*, 254.
5. Huang, Y.; Kinloch, A. *J. Polym.* **1992**, *33*, 1330.
6. Lin, T.; Zhang, X.; Tang, Z.; Guo, B. *Green Chem.* **2015**, *17*, 3301.
7. Venkatanarasimhan, S.; Raghavachari, D. *J. Mater. Chem. A*. **2013**, *1*, 868.
8. Matsuda, S.; Iwata, H.; Se, N.; Ikada, Y. *J. Biomed. Mater. Res.* **1999**, *45*, 20.
9. Wu, J.; Muir, A. D. *J. Food Sci.* **2008**, *73*, 210.
10. Liu, Z.; Luo, Y.; Bai, H.; Zhang, Q.; Fu, Q. *ACS Sustain. Chem. Eng.* **2016**, *4*, 111.
11. Mohamad, Z.; Ismail, H.; Thevy, R. C. *J. Appl. Polym. Sci.* **2006**, *99*, 1504.
12. Lee, H. K.; Ismail, J.; Kammer, H. W.; Bakar, M. A. *J. Appl. Polym. Sci.* **2005**, *95*, 113.
13. Zhang, K.; Misra, M.; Mohanty, A. K. *ACS Sustain. Chem. Eng.* **2014**, *2*, 2345.
14. Kim, J. R.; Netravali, A. N. *ACS Sustain. Chem. Eng.* **2017**, *5*, 4957.
15. Saito, T.; Klinklai, W.; Yamamoto, Y.; Kawahara, S.; Isono, Y.; Ohtake, Y. *J. Appl. Polym. Sci.* **2010**, *115*, 3598.
16. Mateo, C.; Torres, R.; Fernández-Lorente, G.; Ortiz, C.; Fuentes, M.; Hidalgo, A.; López-Gallego, F.; Abian, O.; Palomo, J. M.; Betancor, L.; Pessela, B. C. C.; Guisan, J. M.; Fernández-Lafuente, R. *Biomacromolecules*. **2003**, *4*, 772.
17. Nghia, P. T.; Siripitakchai, N.; Klinklai, W.; Saito, T.; Yamamoto, Y.; Kawahara, S. *J. Appl. Polym. Sci.* **2008**, *108*, 393.
18. Bowen, D. O.; Whiteside, R. C. Epoxy Resins, Advances in Chemistry Series 92; In R. F. Gould (Ed): American Chemical Society: Washington D.C., **1970**, p. 48.
19. Alemdar, A.; Sain, M. *Compos. Sci. Technol.* **2008**, *68*, 557.
20. Brown, T. D.; Dalton, P. D.; Hutmacher, D. W. *Prog. Polym. Sci.* **2016**, *56*, 116.
21. Mascia, L.; Su, R.; Clarke, J.; Lou, Y.; Mele, E. *Eur. Polym. J.* **2017**, *87*, 241.
22. Cacciotti, I.; House, J. N.; Mazzuca, C.; Valentini, M.; Madau, F.; Palleschi, A.; Straffi, P.; Nanni, F. *Mater. Des.* **2015**, *88*, 1109.
23. Cacciotti, I.; Fortunati, E.; Puglia, D.; Kenny, J. M.; Nanni, F. *Carbohydr. Polym.* **2014**, *103*, 22.
24. Deitzel, J.; Kosik, W.; McKnight, S.; Beck Tan, N.; DeSimone, J.; Crette, S. *Polymer*. **2002**, *43*, 1025.
25. Tian, M.; Hu, Q.; Wu, H.; Zhang, L.; Fong, H.; Zhang, L. *Mater. Lett.* **2011**, *65*, 3076.
26. Hamzah, R.; Bakar, M. A.; Khairuddean, M.; Mohammed, I. A.; Adnan, R. *Molecules*. **2012**, *17*, 10974.
27. Costa, L. M. M.; Mattoso, L. H. C.; Ferreira, M. *J. Mater. Sci.* **2013**, *48*, 8501.
28. Davi, C. P.; Galdino, L. F. M. D.; Borelli, P.; Oliveira, O. N.; Ferreira, M. *J. Appl. Polym. Sci.* **2012**, *125*, 2137.
29. Hao, X.; Bai, C.; Huang, Y.; Bi, J.; Zhang, C.; Cai, H.; Zhang, X.; Du, L. *Macromol. Mater. Eng.* **2010**, *295*, 305.
30. Hu, Q.; Wu, H.; Zhang, L.; Fong, H.; Tian, M. *Express Polym. Lett.* **2012**, *6*, 258.
31. Soliman, E. A.; Khalil, A. A.; Deraz, S. F.; El-Fawal, G.; Elrahman, S. A. *J. Food Sci. Technol.* **2014**, *51*, 2425.
32. Corradini, E.; Curti, P.; Meniqueti, A.; Martins, A.; Rubira, A.; Muniz, E. *Int. J. Mol. Sci.* **2014**, *15*, 22438.
33. Wang, N.; Zhang, L. *Polym. Int.* **2005**, *54*, 233.
34. Lodha, P.; Netravali, A. N. *Ind. Crops Prod.* **2005**, *21*, 49.
35. Souzandeh, H.; Johnson, K. S.; Wang, Y.; Bhamidipaty, K.; Zhong, W. H. *ACS Appl. Mater. Interfaces*. **2016**, *8*, 20023.
36. Souzandeh, H.; Wang, Y.; Zhong, W.-H. *RSC Adv.* **2016**, *6*, 105948.
37. Gan, S.-N.; Hamid, Z. A. *Polymer*. **1997**, *38*, 1953.
38. Sam, S. T.; Ismail, H.; Ahmad, Z. *J. Vinyl Addit. Technol.* **2010**, *16*, 238.
39. Lodha, P.; Netravali, A. N. *J. Mater. Sci.* **2002**, *37*, 3657.
40. Lodha, P.; Netravali, A. N. *Compos. Sci. Technol.* **2005**, *65*, 1211.
41. Doszlop, S.; Vargha, V.; Horkay, F. *Period. Polytech. Chem. Eng.* **1978**, *22*, 253.
42. Müller, V.; Piai, J. F.; Fajardo, A. R.; Fávaro, S. L.; Rubira, A. F.; Muniz, E. C. *J. Nanomater.* **2011**, *2011*, 1.
43. Guinesi, L. S.; Cavalheiro, É. T. G. *Thermochim. Acta.* **2006**, *444*, 128.
44. Tillekeratne, M.; Easteal, A. J. *Polym. Int.* **2000**, *49*, 127.
45. De Almeida, C. B.; Corradini, E.; Forato, L. A.; Fujihara, R. *Polímeros*. **2018**, *28*, 30.
46. Tihminlioglu, F.; Atik, İ. D.; Özen, B. *J. Food Eng.* **2010**, *96*, 342.

47. Santosa, F. X. B.; Padua, G. W. *Cereal Chem. J.* **2000**, *77*, 459.
48. Magoshi, J.; Nakamura, S.; Murakami, K. I. *J. Appl. Polym. Sci.* **1992**, *45*, 2043.
49. Oliviero, M.; Di Maio, E.; Iannace, S. *J. Appl. Polym. Sci.* **2010**, *115*, 277.
50. Tian, H.; Liu, D.; Yao, Y.; Ma, S.; Zhang, X.; Xiang, A. *J. Food Sci.* **2017**, *82*, 2926.
51. Copeland, J.; Thames, S. F. *J. Coat. Technol.* **1994**, *66*, 59.
52. Li, C.; Wan, J.; Pan, Y.-T.; Zhao, P.-C.; Fan, H.; Wang, D.-Y. *ACS Sustain. Chem. Eng.* **2016**, *4*, 3113.
53. Kim, J. R.; Sharma, S. *Ind. Crops Prod.* **2012**, *36*, 485.